

Vinay K Sharma, S Radhakrishnan, and S Shrivastava. Three-dimensional trans-esophageal Echocardiographic Evaluation of Atrial Septal Defects: A Pictorial Essay. Images Paediatr Cardiol. 2011 Jul-Sep; 13(3): 1–18.



Images Paediatr Cardiol. 2011 Jul-Sep; 13(3): 1–18.

PMCID: PMC3232598

Three-dimensional trans-esophageal Echocardiographic Evaluation of Atrial Septal Defects: A Pictorial Essay

Vinay K Sharma, S Radhakrishnan, and S Shrivastava
Fortis Escorts Heart Institute and Research Centre Ltd., Okhla road, New Delhi-
110025, India.

Contact information: Vinay Kumar Sharma, Consultant Cardiologist, Fortis Escorts
Heart Institute and Research Centre Ltd., Okhla road, New Delhi-110025, India.
Email: drvinay123@indiatimes.com

Copyright : © Images in Paediatric Cardiology

This is an open-access article distributed under the terms of the Creative Commons
Attribution-Noncommercial-Share Alike 3.0 Unported, which permits unrestricted use,
distribution, and reproduction in any medium, provided the original work is properly
cited.

Abstract

This pictorial assay illustrates the methodology of evaluating the atrial septal defects by three dimensional transesophageal echocardiography with the help of representative images. The article starts by discussing the technical details of how to acquire and crop the dataset to reconstruct the transesophageal three dimensional echocardiographic images of the inter atrial septum. Next, the anatomical details of the normal inter atrial septum are illustrated, followed by representative examples of all the possible defects of inter atrial septum. All the images have been reproduced in a uniform pattern which is similar to the view of the inter atrial septum that is seen in the real life situation by the surgeon.

MeSH: echocardiography, atrial septal defect

Abbreviations used in the article

TTE: Trans Thoracic Echocardiography.

2D TTE: Two Dimensional Trans Thoracic Echocardiography.

TEE: Trans Esophageal Echocardiography.

2D TEE: Two Dimensional Trans Esophageal Echocardiography.

3D TEE: Three Dimensional Trans Esophageal Echocardiography.

ASD: Atrial Septal Defect.

IAS: Inter Atrial Septum.

RA: Right Atria.

RV: Right Ventricle.

TV: Tricuspid Valve.

SVC: Superior Vena Cava.

IVC: Inferior Vena Cava.

CS: Coronary Sinus.

The development of three dimensional transesophageal echocardiography (3D TEE) has thrown up several exciting possibilities and evaluation of atrial septal defects (ASDs) is one of the most promising among these possibilities. ASD is the most common congenital heart disease in adult and adolescents, with the ostium secundum variety alone accounting for 30-40 % of all congenital heart diseases seen in this age group.¹

In a subset of patients with ostium secundum atrial septal defects, percutaneous closure by a septal occluder devices can be offered as an alternative to cardiac surgery.²⁻⁵ Echocardiography plays a very important role in identifying these patients. Two dimensional transesophageal echocardiography (2D TEE) is by far very superior to two dimensional transthoracic echocardiography (2D TTE) or three dimensional transthoracic echocardiography (3D TTE) to evaluate an ASD, as transesophageal echocardiography (TEE) is not hindered by the problem of poor echocardiographic windows.⁶⁻⁸ In fact, an ASD is never taken up for device closure without first doing a TEE study to assess adequacy of its margins to hold the device.

3D TEE is further superior to 2D TEE as it provides all the needed information in a single view, which otherwise would take a series of 2D TEE views, leading to inter- and intraobserver variation in assessment of the ASD.⁹

This pictorial assay explains the technique of acquisition and cropping of three dimensional (3D) datasets to produce 3D images of interatrial septum (IAS), followed by representative examples of normal IAS and its defects. As of today, the use of matrix array probes is the standard way of obtaining the real-time three dimensional echocardiographic images, and all the images shown in this article have been acquired with a fully sampled matrix array 3D TEE probe (iE, Philips Medical Systems, USA).

Technical Considerations and Cropping Sequence

The details of methodology to create 3D TEE images of the IAS is beyond the scope of this article and can be found elsewhere.¹⁰ However, certain important technical issues must be highlighted.

The first technical issue to be addressed is about the choice of the echocardiographic view to obtain a three dimensional dataset. Theoretically, any cardiac structure can be imaged from a single full volume 3D dataset acquired from any probe position. Practically, we have found the dataset acquired from the mid esophageal basal long axis (or bicaval) view to be most useful to reconstruct 3D images of the atrial septal defects. This view is acquired from midesophageal position, after electronically rotating the probe by 90°. This dataset contains, from anterior to posterior, right atrial free wall, right atrial cavity, IAS and left atrial cavity. Removal of the RA free wall brings in view IAS from right atrial perspective. This en face view of IAS from right atrial perspective is similar to the view of inter atrial septum which will be seen by the surgeon.

The second important issue is to avoid stitch artifacts. The full volume data sets are compiled by “stitching together” four narrow pyramidal scans obtained over four consecutive heartbeats. Stitch artifacts result when the position of the heart changes in between any of these four cycles. The most common cause of this problem is a suboptimal ECG signal, as the datasets are acquired by ECG gating. The second most common cause of stitch artifacts is the translational movement of the heart due to respiration. Translational movement of the heart can be avoided by acquiring the dataset during suspended respiration. The images given in this article have been obtained during suspended respiration.

The third, and probably the most important consideration in obtaining good quality 3D images, is to have optimal gain settings before the acquisition of the dataset. Low

gain settings leads to echo dropouts and these parts cannot be seen in 3D images. On other hand, high gain settings lead to blurring of fine structural details. It is not possible to define an optimal gain setting which can be applied universally in every patient and optimal gain setting has to be defined for each individual patient. In our laboratory, we keep the gain setting in mid range and the first dataset is cropped immediately after its acquisition. If there are echo dropouts, then the gain is further increased before acquiring subsequent datasets. Similarly, if the anatomical boundaries are getting blurred, then gain is decreased before acquiring the next dataset. Figure 1 illustrates the importance of having optimal gain settings before acquisition of 3D datasets.

Figure 1 Picture A, B and C are 3D TEE images of IAS from RA perspective and shows the importance of the maintaining proper gain settings during the image acquisition and the fact that it has to be individualized for every patient. Picture A is taken after optimal gain setting and shows centrally placed secundum ASD with good surrounding margins. Picture B has been taken after decreasing the gain and it can be seen that now echo dropouts have appeared near the postero-inferior margin of the defect. Picture C has been taken after increasing the gain and shows that it completely blurs the anatomical boundaries and no defect can be seen.



Once a 3D dataset is acquired, it must be cropped to visualize inter atrial septum. The aim of cropping the 3D dataset is to create a view of inter atrial septum which is similar to the view to be seen by the surgeon. Figure 2 illustrates the sequence of cropping a 3D dataset to create this “real life” view of inter atrial septum.

Representative examples of various types of ASDs

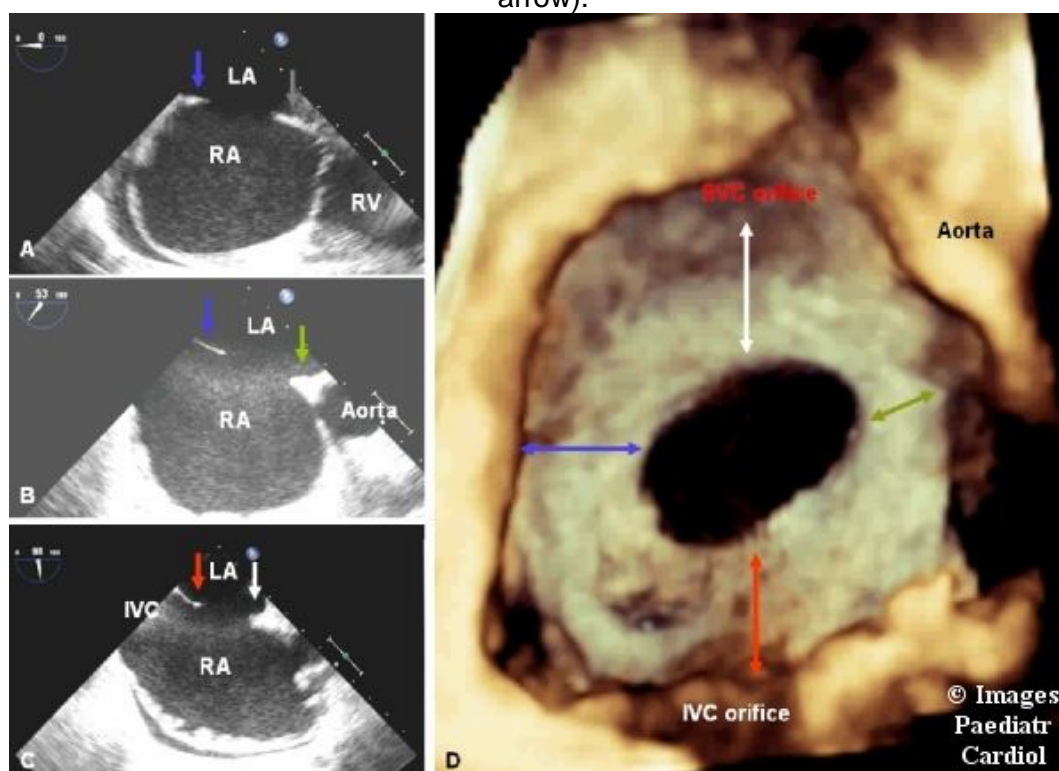
Example 1: Figure 3 displays images of a centrally situated secundum ASD. This ASD has good surrounding margins and thus is ideal to understand the nomenclature of the margins of fossa ovalis ASD. The names of the margins of an ASD are designated according to the structures in their vicinity.¹⁰ The margin between the defect and SVC is called the SVC margin, the margin between the defect and IVC is called the IVC margin, the margin at the crux is called the atrioventricular (AV) septal margin, the margin between defect and the ascending aorta is called the aortic margin and the margin between the defect and the superior wall of atrium near the right upper pulmonary vein is called the atrial margin. The location of these margins of the ASD has been illustrated in figure 3.

Figure 2 Picture A shows the raw 3D dataset which has been acquired in basal long axis view (bicaval view). Picture B displays the dataset after the initial cropping has removed the RA free wall and the tricuspid valve comes in view (red arrows).

Picture C displays the dataset after further cropping, till aorta comes in view. Picture D displays the dataset after further cropping, till the image of IAS from right atrial perspective comes in view. Several anatomical features of IAS can be seen in great detail. The oval depression in the central part of the IAS is called fossa ovalis. It is the thinnest part of the IAS (IAS itself is very thin, being only 2 mm thick). The fossa ovalis is bounded by a thicker rim of tissue, called limbus of fossa ovalis (red arrows). It is most pronounced above and on the side of the fossa ovalis and is deficient in its inferior part. The opening of the coronary sinus can be seen to the left of the limbus. Aorta (white arrows), SVC and IVC are also seen in this view. It is important to memorize the position of SVC, IVC, aorta and TV in relation to the IAS, because these structures are used as landmarks to define the margins of the ASD.

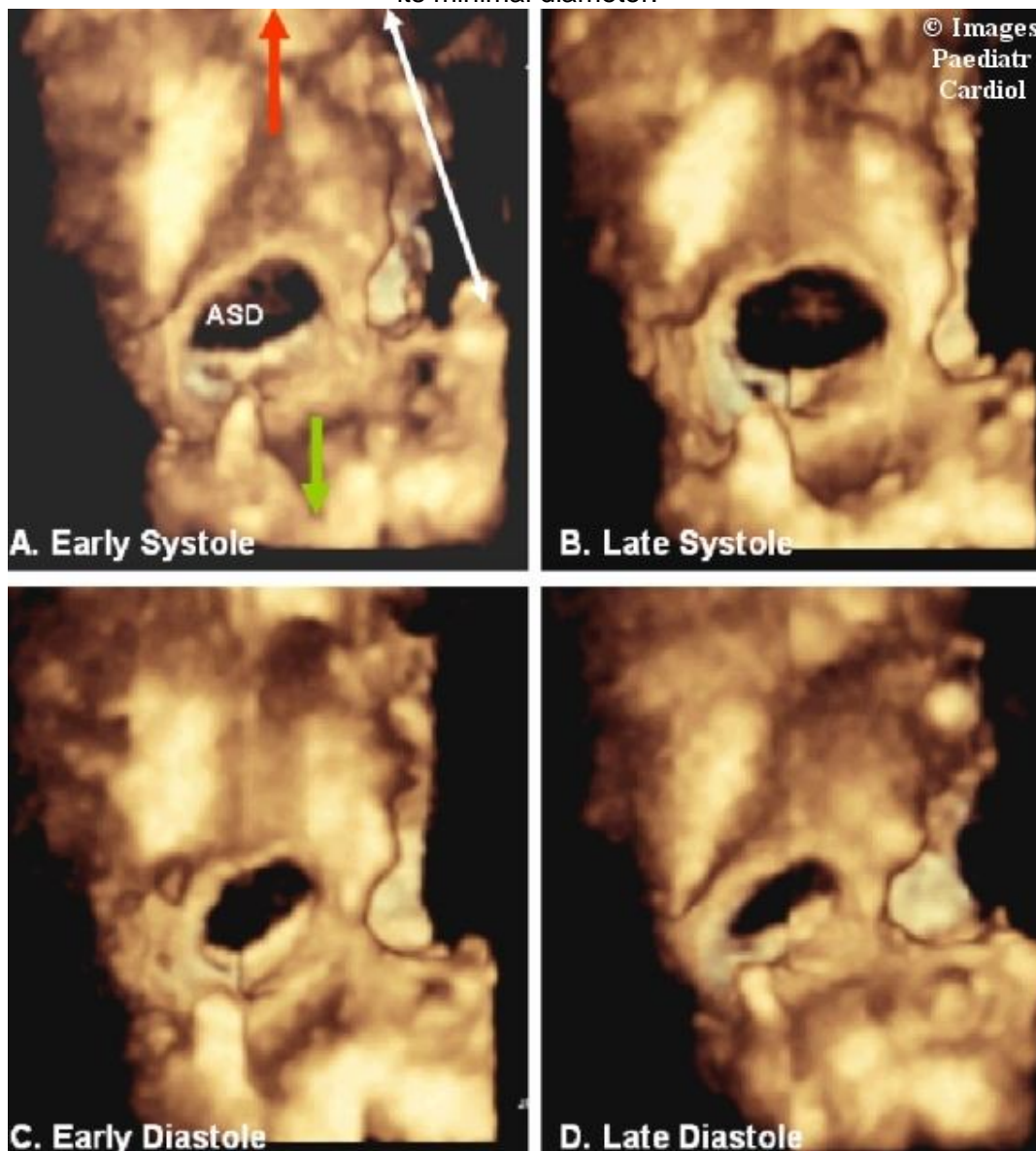


Figure 3 Picture A, B and C are 2D TEE images of a centrally situated secundum type ASD. Picture A is four chamber view and shows AV septal margin (grey arrow) and atrial margin (blue arrow). Picture B is basal short axis view and shows the retro aortic margin (green arrow). Picture C is the basal long axis (bicaval view) and shows the SVC margin (white arrow) and IVC margin (red arrow). Picture D is three dimensional en-face view of inter atrial septum from RA perspective and shows all the margins of the ASD in a single image . These margins are, clockwise from top, SVC margin (white double headed arrow) , aortic margin (green double headed arrow), IVC margin (red double headed arrow) and atrial margin (blue double headed arrow).



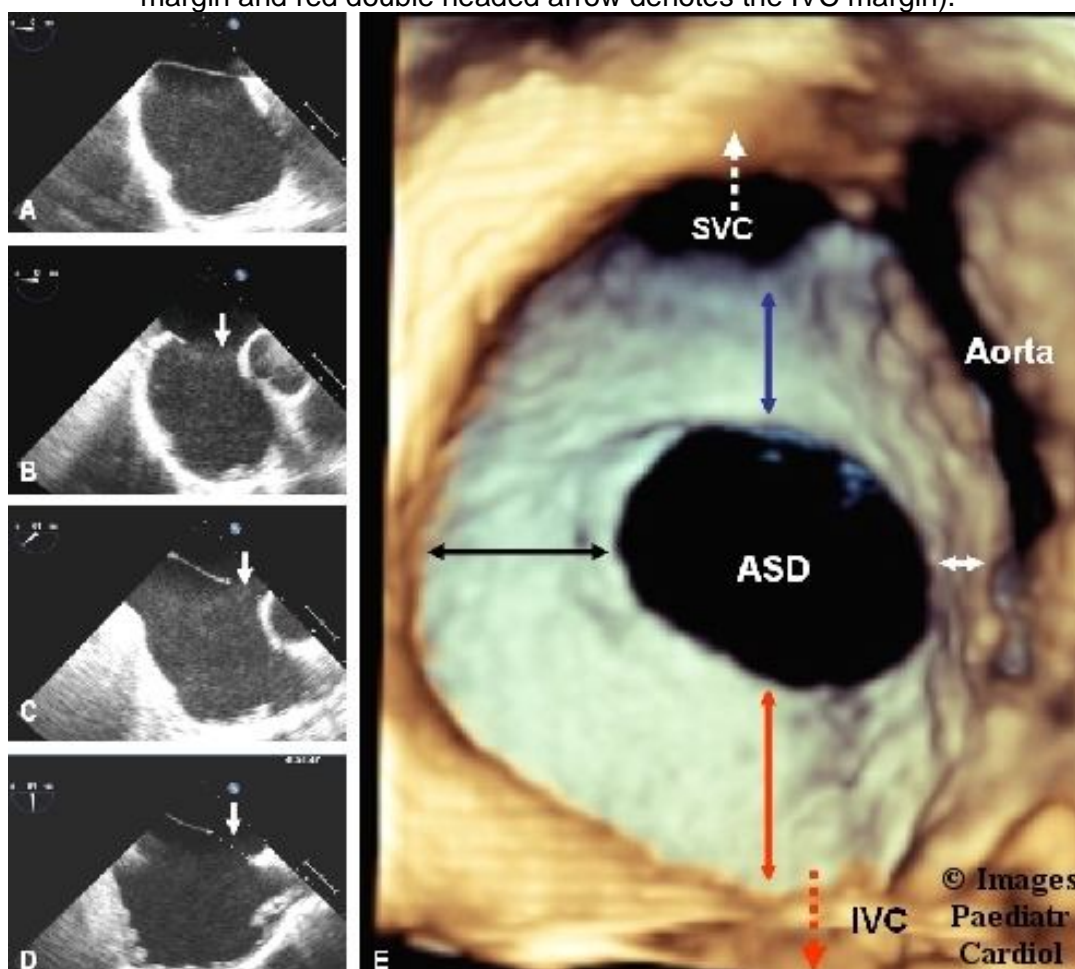
Example 2: Figure 4 illustrates the changes in surface area of a secundum ASD during various phases of the cardiac cycle. The surface area of the ASD changes significantly during the cardiac cycle, with a maximum size in late ventricular systole and a minimum size in late left ventricular diastole.¹¹ These changes in the shape and the size of the ASD are caused by contraction of the defect as well as the movement of the heart.^{12,13} These changes are better appreciated by 3D TEE , while the 2D echocardiography can underestimate the size of defect as the imaging plane may not be through the maximal diameter of the defect.¹⁴

Figure 4 Picture A, B, C and D are 3D TEE view of IAS from the RA perspective. Picture A has been labeled to depict the structures being seen. Red arrow denote the position of SVC, green arrow denotes position of IVC and double headed white arrow denotes the position of aorta. The picture B is of late systole, showing the maximal diameter of ASD. Picture C is from early diastole and shows that the diameter of the ASD has started decreasing. Picture D is from late diastole when the ASD reaches its minimal diameter.



Example 3: Figure 5 shows the most common type of secundum ASD encountered in clinical practice. These ASDs have deficient aortic margins, while the other three margins i.e. SVC, IVC and atrial margins, are big enough to grip the device. These defects can be closed with septal occlude devices but require considerably more operator experience and also carry more chances of complications, including that of device migration.

Figure 5 Picture A, B, C and D are 2D TEE images of an ASD with deficient aortic margin. Picture A is four chamber view from mid esophageal position and shows an intact IAS. Picture B is four chamber view taken after pulling the probe to high esophageal location and now the septal defect can be seen. This implies that the defect is superiorly situated. Picture C is basal short axis view and shows that the retro aortic margin of the defect is absent. Picture D is basal long axis (bicaval) view. The defect is still being seen but the defect size is less than that being seen in picture B, thus suggesting that the defect is anteriorly situated. So, the defect is anteriorly and superiorly situated and the aortic margins are deficient. Picture E is 3D TEE image of the ASD from RA perspective. The aortic margin (white double headed arrow) is deficient, while all other margins are quite robust (blue double headed arrow denotes the SVC margin, black double headed arrow denotes the atrial margin and red double headed arrow denotes the IVC margin).



Example 4: Figure 6 shows a 3D TEE image from a patient with two secundum ASDs. Multiple ASDs are a relatively uncommon occurrence. In a series of 190 patients, only 7.3 % patients were found to be having multiple atrial septal defects.¹⁵ The patients with multiple ASDs require all defects to be individually evaluated to decide adequacy of their margins for device closure. Further, the margin between the two defects is also to be evaluated, to decide whether to use one device or to use two separate devices to close them. It has been suggested that the rim between the two defects should at least be 7 mm to allow the deployment of two devices.¹⁶ In the example given here, a single 3D image of IAS contains all the required information. In this case, both defects had good surrounding margins and they were separated by

a thick rim of tissue. These ASDs were successfully closed with two separate septal occlude devices.

Example 5: Figure 7 displays a fossa ovalis ASD, which is coexisting with an aneurysm of inter atrial septum. It can be very difficult to define the exact relation of the ASD to the neurismal part of the septum by 2D imaging. Three dimensional imaging is of great help in profiling the ASD and it's relation to the neurismal part of inter atrial septum.

Figure 6 Picture A, B, C and D are 2D TEE images of multiple ASDs. Picture A is four chamber view, showing the presence of two separate ASDs, labeled as number 1 and 2, with ASD number 2 being nearer to the aorta. Picture B is basal short axis view and confirms the presence of two separate ASDs. Picture C is bicaval view and it shows only one ASD, suggesting that one of the ASD (ASD number 2) is situated in a more anterior plane. Picture D is the 3D TEE image of IAS from RA perspective showing relative position of both the ASDs. It can be seen that both the ASDs have very stout IVC margin and are also separated by a good amount of tissues, making them suitable for closure by two separate devices. The black arrows show the Eustachian valve.

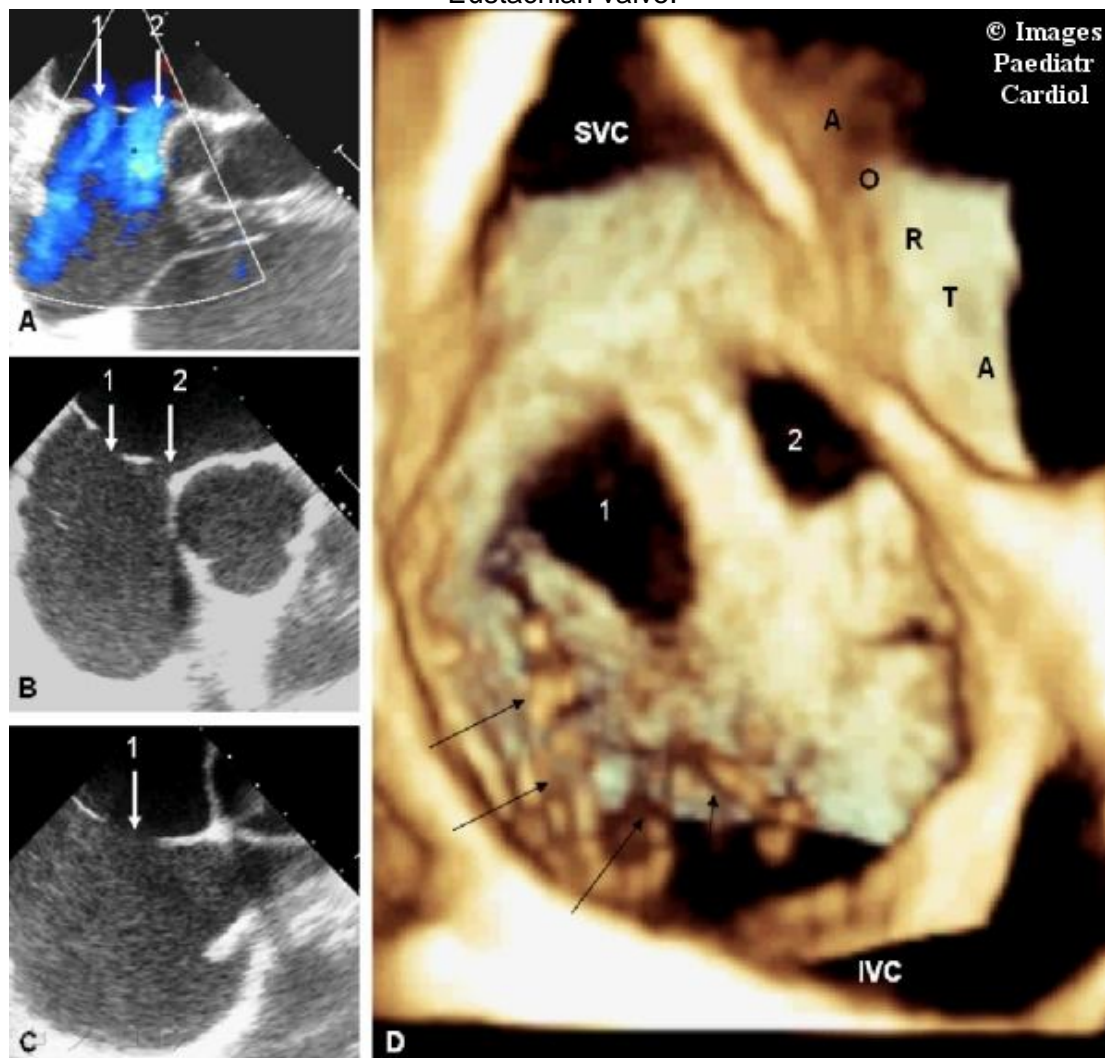
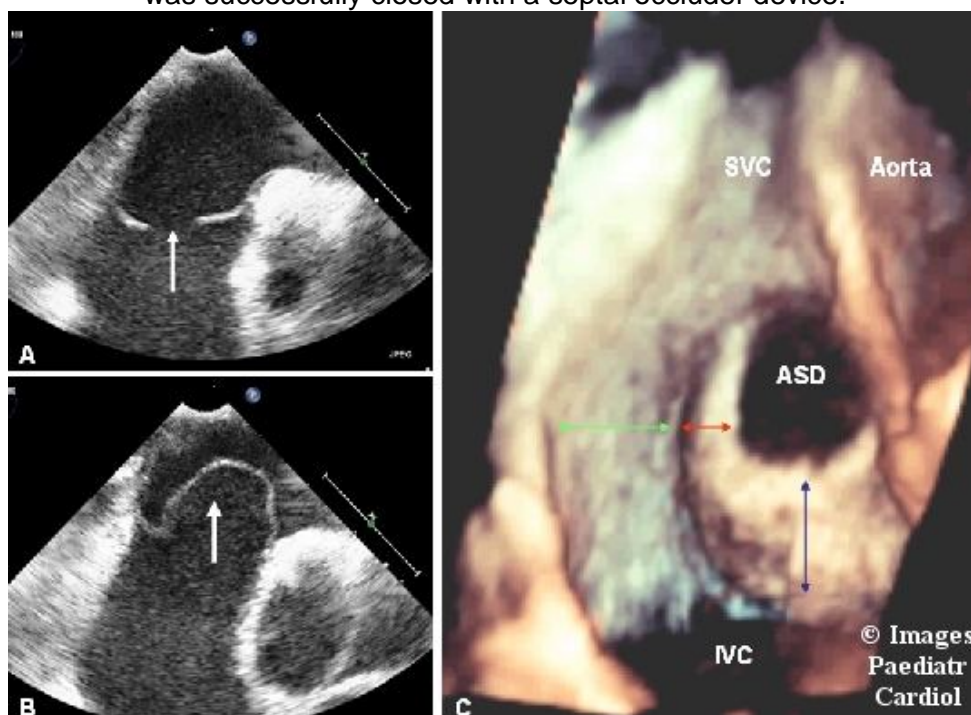


Figure 7 Picture A and B are 2D TEE four chamber images. Picture A shows the presence of a fossa ovalis ASD. Picture B is from same probe position and shows large aneurysm of inter atrial septum (white arrow). Picture C is a 3D TEE image of the IAS from RA perspective and very vividly demonstrates the relative position of the aneurysm and the ASD. The almost entire IVC margin (blue double headed arrow) and anterior part of the atrial margin (red double headed arrow) is aneurysmal. Remaining part of the atrial margin (green double headed arrow) is normal. This ASD was successfully closed with a septal occluder device.



Example 6: Figure 8 shows another situation which is even more complex than the examples seen so far. This patient had multiple ASDs which were coexisting with an aneurysm of interatrial septum. In such cases, 3D imaging can be invaluable to define the exact relation of all the abnormalities of the structure of IAS.

Example 7 and 8: Figure 9 shows SVC type sinus venosus defect, which is the most common variety of sinus venosus defects seen in adults. Figure 10 shows the IVC type sinus venosus defect, which is the rarest variety of sinus venosus defects seen in the adults. Sinus venosus defects are diagnosed by the triad of presence of intact fossa ovalis, presence of a muscular rim between the defect and the fossa and overriding of the vena cava by the IAS. The intact muscular border between the fossa ovalis and the septal defect can be easily identified by 3D TEE and holds the key to diagnose sinus venosus defects on 3D imaging.¹⁷

Figure 8 Picture A and B are 2D TEE images of inter atrial septum. Picture A is four chamber view, showing the presence of an aneurysm of IAS. Picture B is basal long axis (bicaval) view, showing two separate defects (white arrows) of inter atrial septum. Careful scan of the image also shows that the second defect is situated nearer to IVC, in aneurysmal part of the IAS. Picture C is a 3D TEE image of ASD from RA perspective. The almost entire IVC margin of the larger defect is aneurysmal and the smaller ASD is situated in this aneurysmal part. The presence of the funnel around the second defect helps in differentiating the defect from an echo dropout.

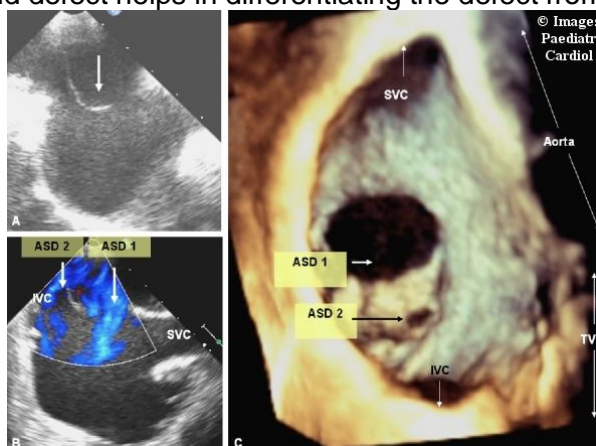


Figure 9 Picture A, B and C are 2D TEE images of an SVC type sinus venosus defect. Picture A is four chamber view from mid esophageal position and does not show any defect. However, this view shows the flap of foramen ovale (white arrow) which rules out the possibility of presence of a fossa ovalis type defect. Picture B is four chamber view taken from a higher esophageal position and reveals the presence of a defect of atrial septum (white arrow). Picture C is basal long axis view and shows the SVC type defect (red double headed arrow) with straddling of IAS by SVC. Picture D is a 3D TEE image of the defect. A muscular rim between the defect and fossa ovalis confirms the diagnosis of sinus venosus type defect. The defect is situated very high up near the SVC orifice and the lower half of the IAS had to be excluded from the dataset (white double headed arrow) to visualize the defect.

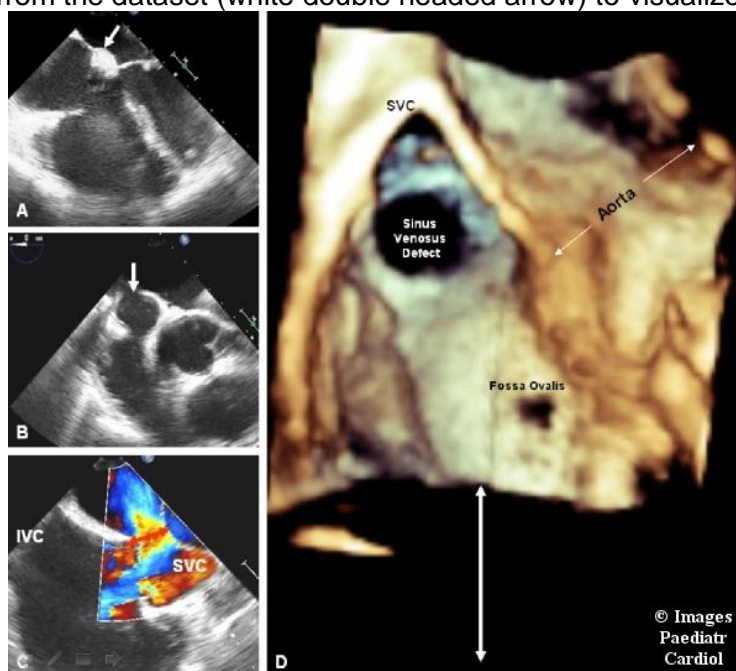
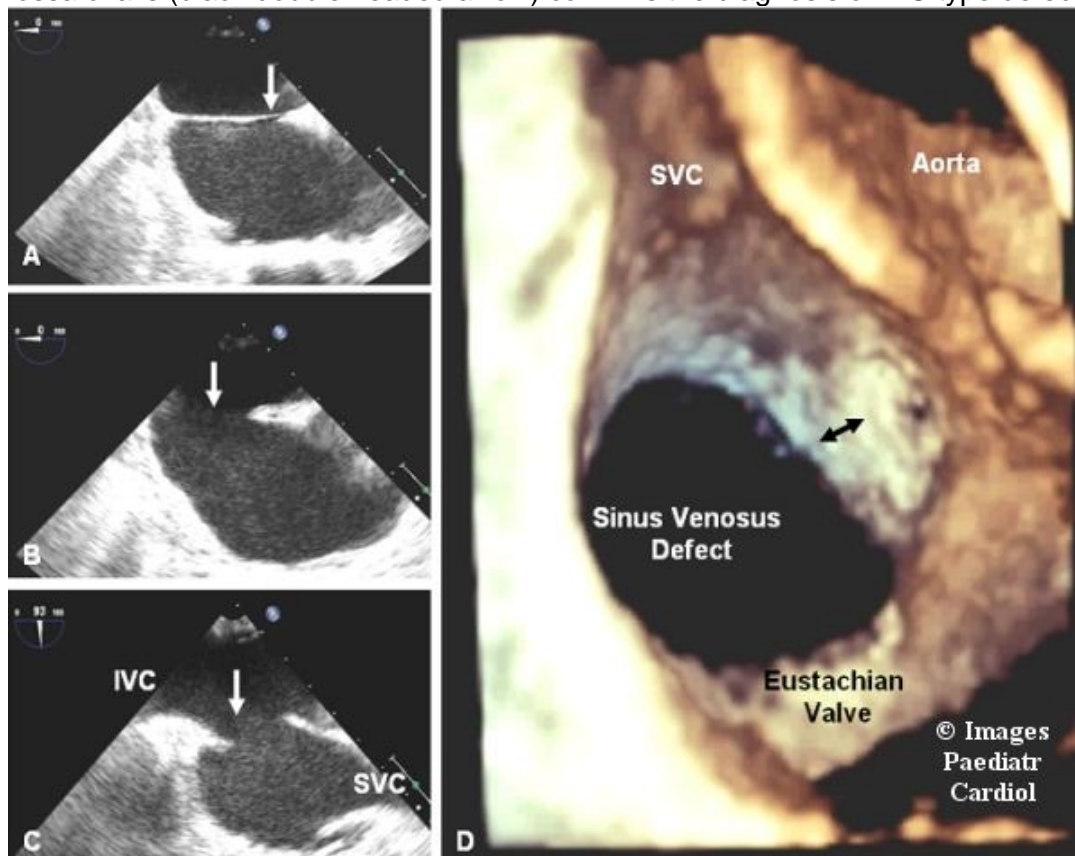


Figure 10 Picture A, B and C are 2D TEE images of an IVC type sinus venosus defect. Picture A is four chamber view from mid esophageal position and does not show any defect. However, this view shows the flap of foramen ovale (white arrow) which rules out the possibility of presence of a fossa ovalis type defect. Picture B is the 4 chamber view taken from a lower esophageal position and reveals the presence of a defect of atrial septum (white arrow). Picture C is basal long axis view and shows the IVC type defect (white arrow) with straddling of the IAS by IVC. Picture D is a 3D TEE image of the defect. A muscular rim between the defect and fossa ovalis (black double headed arrow) confirms the diagnosis of IVC type defect.



Example 9: Three dimensional imaging of the IAS has a potentially important role in planning the procedures involving septal puncture. Figure 11 shows an example of an aneurysm of inter atrial septum in a patient with severe rheumatic mitral stenosis. The TEE was done as part of routine diagnostic evaluation prior to percutaneous trans mitral commissurotomy (PTMC). In this case, 3D images demonstrated the presence of aneurysm of IAS and its precise localization helped in planning appropriate precaution during septal puncture.

Example 10: Figure 12 shows a post- PTMC atrial septal defect. PTMC is a very commonly performed procedure with close to 8000 PTMC procedures having been carried out in India in 2005 (this study included the data from only 71 centers and actual number is likely to be much higher).¹⁸ The creation of an atrial septal defect (ASD) is inherent in the antegrade PTMC approach , and its incidence is as high as 67% at 48 hours.¹⁹ Most of these defects are small and close spontaneously over next one year.²⁰ However 3-15% of patients do develop significant atrial shunts (defined as a pulmonary-to-systemic flow of > 1.3:1).^{20,21} The shape of these ASDs varies, depending on the cross-sectional profile of the deflated balloon.

Example 11: Figure 13 shows an example of quantitative measurements of the ASD size. The 3D quantification of the ASD offers several advantages over 2D measurements. 3D imaging shows the entire defect in a single view, allowing the

operator to choose the maximal diameter with certainty. The 2D imaging, on the other hand, requires a series of views to measure the defect and can miss the maximal diameter of the defect as the operator can evaluate only few of infinite number of possible 2D planes. This becomes even more important in defects which are not spherical in shape.

Figure 11 Picture A is the image of the mitral valve in so called surgeon' view (mitral valve being seen from LA perspective with aorta positioned in 11 o clock position). The red arrow denotes the fish mouth appearance of the stenotic mitral valve. Picture B shows the coexisting aortic stenosis and red arrow points to the stenotic opening of the aortic valve. Picture C is 2D TEE image in basal short axis view. The white arrow points to the aneurysm of inter atrial septum. Picture D is 3D TEE image of IAS from RA perspective. The white arrow points to the location of the aneurysm of inter atrial septum.



Figure 12 These pictures are from a patient who has undergone PTMC for rheumatic mitral stenosis. Picture A is 2D TEE four chamber image and shows the presence of left to right shunt across IAS. Picture B is a 3D TEE image of the ASD and shows an atrial septal defect, situated at superior border of the fossa ovalis. The shape of the post PTMC atrial septal defects is dependent on the cross sectional profile of the balloon and the angle at which the balloon penetrates the septum. In this case the defect is elongated in shape. Picture C is 3D TEE color flow image of IAS from the RA perspective and confirm the presence of the atrial septal defect. Picture D is same as picture C but taken after suppression of the color flow. The similarity of the shape in picture B confirms that it is actually the same defect as being seen in picture B.

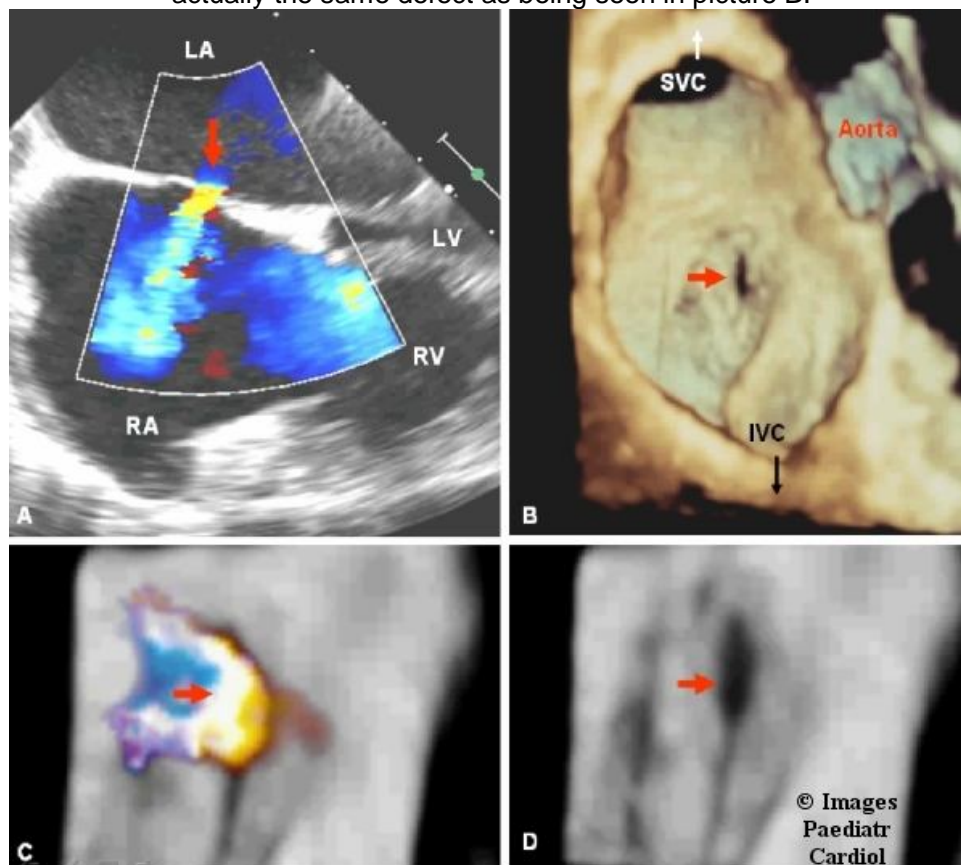
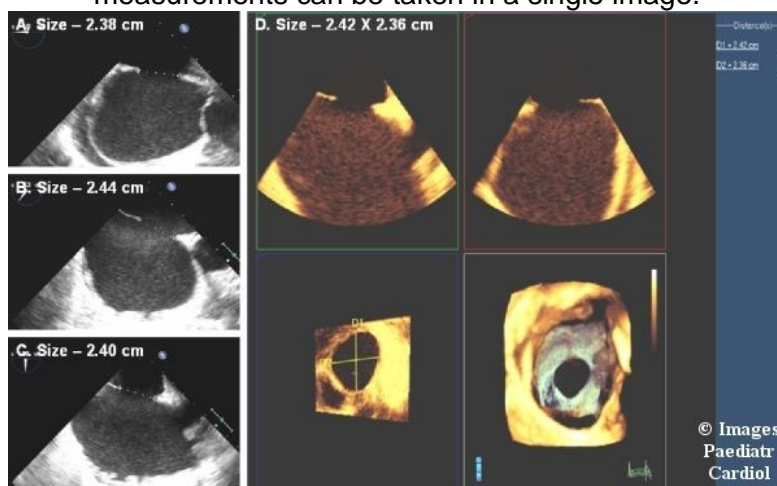


Figure 13 Picture A, B and C shows measurements of an ASD by 2D TEE imaging. Picture A is 4 chamber view and the diameter measured in this view is the horizontal diameter and corresponds to the D2 measurement in the 3D image. Picture B shows diameter in basal short axis image. Picture C is the bicaval view and the diameter shown in this image is the vertical diameter and corresponds to D1 diameter in the 3D image. Picture D shows 3D TEE image of the defect and shows that all measurements can be taken in a single image.



Example 12: The examples seen so far emphasize the usefulness of 3D TEE imaging in pre-device closure assessment of the size of the defect and adequacy of its margins to grip the device. However, 3D TEE also has a potentially very useful role during the procedure of device closure. Figure 14 shows the images taken during the device deployment to close a fossa ovalis defect. It rapidly confirms the proper positioning of the device across all the margins. A single 3D TEE image can provide the answer to the every question that arises before and after the deployment of the device. 3D imaging can tell whether the device is excessively mobile or whether it is encroaching onto AV valves or pulmonary veins or SVC or IVC orifices.

Figure 14 Figure A, B and C are 3D TEE images of the inter atrial septum from RA perspective, taken during the closure of a secundum ASD with a septal occluder device. Picture A shows the positioning of the catheter across the defect. Picture B shows the image of the device after it has been opened, but has not yet been released from the catheter. This image is used to evaluate the proper positioning of the device and it's relation to the surrounding margins as well as the orifices of pulmonary veins, SVC and IVC. Picture C is taken after release of the device from the catheter and confirms that the device is properly positioned. A device which is properly positioned and firmly gripping all the margins of the defect should not have excess mobility.



Conclusion

The examples given so far emphasize the fact that 3D echocardiography provides the most precise answer to the most important question – “is this defect suitable for trans catheter closure”. This assessment includes number, size and shape of the defect as well as the size of the margins of the defect. 3D TEE imaging has the potential to significantly cut down the time taken to assess the likely problems before releasing the device from the catheter, as it can show the relation of the device to the defect in a single image ,which otherwise would take a series of 2D views.

References

1. Dickinson DF, Arnold R, Wilkinson JL. Congenital heart disease among 160480 live born children in Liverpool 1960 to 1969- Implications for surgical treatment. *Br Heart J.* 1981;46:55–62. [PMCID: PMC482602][PubMed: 7272113]
2. Rome JJ, Keane JF, Perry SB, Spevak PJ, Lock JE. Double umbrella closure of atrial defects. Initial clinical applications. *Circulation.* 1990;82:751–8. [PubMed: 2394001]
3. Das GS, Voss G, Jarvis G, Wyche K, Gunther R, Wilson RF. Experimental atrial septal defect closure with a new, transcatheter, self-centering device. *Circulation.* 1993;88:1754–64. [PubMed: 8403322]
4. Chan KC, Godman MJ. Morphological variations of fossa ovalis atrial septal defects (secundum): feasibility for transcatheter closure with the clam-shell device. *Br Heart J.* 1993;69:52–5. [PMCID: PMC1024917][PubMed: 8457395]
5. Hellenbrand WE, Fahey JT, McGowan FX, Weltin GG, Kleinman CS. Transoesophageal echocardiographic guidance of transcatheter closure of atrial septal defect. *Am J Cardiol.* 1990;66:207–13. [PubMed: 2371953]
6. Peter H, Michael S, Burkhart A L, Julia P, Stefan E, Peter K, Hans-Joachim K. Detection of ostium secundum atrial septal defects by transoesophageal cross-sectional echocardiography. *Br Heart J.* 1983;49:350–8. [PMCID: PMC481312][PubMed: 6830669]
7. Morimoto K, Matsuzaki M, Tohma Y, Ono S, Tanaka N. Diagnosis and quantitative evaluation of secundum-type atrial septal defect by transesophageal Doppler echocardiography. *Am J Cardiol.* 1990;66:85–91. [PubMed: 2360537]
8. Su CH, Weng KP, Chang JK, Lin CC, Hwang YT, Lee CL, Chien KY, Chen FL, Yu CK, Liu WS, Huang T TC, Hsieh KS. Assessment of Atrial Septal Defect - Role of Real-Time 3D Color Doppler Echocardiography for Interventional Catheterization. *Acta Cardiol Sin.* 2005;21:146–52.
9. Sharma V, Radhakrishnan S, Shrivastava S. Transesophageal Echocardiographic Evaluation of Atrial Septal Defects - How to Explore the Third Dimension. *Indian Heart J.* 2009;61:328–334. [PubMed: 20635734]
10. Shrivastava S, Radhakrishnan S. Echocardiographic anatomy of atrial septal defect: “nomenclature of the rims” *Indian Heart J.* 2003;55:88–9. [PubMed: 12760597]
11. Gu X, Han YM, Berry J, et al. A new technique for sizing of atrial septal defects. *Catheter Cardiovasc Interv.* 1999;46:51–7. [PubMed: 10348567]
12. Lange A, Walayat M, Turnbull CM, Palka P, Mankad P, Sutherland GR, Godman MJ. Assessment of atrial septal defect morphology by transthoracic three dimensional echocardiography using standard gray scale and Doppler myocardial imaging techniques: comparison with magnetic resonance imaging and intraoperative findings. *Heart.* 1997;78:382–9. [PMCID: PMC1892258][PubMed: 9404256]
13. Franke A, Kühl HP, Rulands D, Jansen C, Erena C, Grabitz RG, Däbritz S, Messmer BJ, Flachskampf FA, Hanrath P. Quantitative analysis of the morphology of secundum-type atrial septal defects and their dynamic change using transesophageal three-dimensional echocardiography. *Circulation.* 1997;96(9 Suppl):II-323–7.
14. Maeno YV, Benson LN, McLaughlin PR, Boutin C. Dynamic morphology of the secundum atrial septal defect evaluated by three dimensional transoesophageal echocardiography. *Heart.* 2000;83:673–677. [PMCID: PMC1760878][PubMed: 10814628]
15. Podnar T, Martanovic P, Gavora P, Masura J. Morphological variations of secundum-type atrial septal defects: feasibility for percutaneous closure using Amplatzer septal occluders. *Catheter Cardiovasc Interv.* 2001;53:386–91. [PubMed: 11458420]

Vinay K Sharma, S Radhakrishnan, and S Shrivastava. Three-dimensional trans-esophageal Echocardiographic Evaluation of Atrial Septal Defects: A Pictorial Essay. *Images Paediatr Cardiol*. 2011 Jul-Sep; 13(3): 1–18.

16. Cao Q, Radtke W, Berger F, Zhu W, Hijazi ZM. Transcatheter closure of multiple atrial septal defects. Initial results and value of two- and three-dimensional transoesophageal echocardiography. *Eur Heart J*. 2000;21:941–7.[PubMed: 10806019]

17. al Zaghal AM, Li J, Anderson RH, Lincoln C, Shore D, Rigby ML. Anatomical criteria for the diagnosis of sinus venosus defects. *Heart*. 1997;78:298–304. [PMCID: PMC484934][PubMed: 9391294]

18. Chaturvedi V, Talwar S, Airan B, Bhargava B. Interventional cardiology and cardiac surgery in India. *Heart*. 2008;94:268–274.[PubMed: 18276813]

19. Manjunath CN, Prabhavathi, Srinivas KH. Incidence and Predictors of Atrial Septal Defect after Percutaneous Transvenous Mitral Commissurotomy - A Transesophageal Echocardiographic Study. *Indian Heart Journal*. 2009;61:113.[PubMed: 19729704]

20. Ishikura F, Nagata S, Yasuda S, Yamashita N, Miyatake K. Residual atrial septal perforation after percutaneous transvenous mitral commissurotomy with Inoue balloon catheter. *Am Heart J*. 1990;120:873–878.[PubMed: 2220540]

21. Cequier A, Bonan R, Serra A, Dyrda I, Crépeau J, Dethy M, Waters D. Left-to-right atrial shunting after percutaneous mitral valvuloplasty - Incidence and long-term hemodynamic follow-up. *Circulation*. 1990;81:1190–1197.[PubMed: 2317902]

© Images in
Paediatric Cardiology
(1999-2012)

